

# Development of a magnetic levitation vibration isolator using inclined permanent magnet springs

Yann Frizenschaf, Siobhan Giles, Jack Miller, Thomas Pitman,  
Christopher Stapleton, Benjamin Cazzolato and Will Robertson

School of Mechanical Engineering, University of Adelaide, Adelaide, Australia

## ABSTRACT

Vibration isolation systems incorporating linear mechanical springs exhibit the undesirable characteristic of changing resonance frequency with changing payload mass. Previous research at the University of Adelaide and elsewhere has demonstrated the theoretical feasibility of vibration isolation devices utilising magnetic springs as a means of achieving a constant resonance frequency across a range of payload masses due to their nonlinear force-displacement relationship. A conceptual prototype design is presented for a levitating magnet vibration isolation device which aims to achieve a load-independent resonance frequency across a range of payload masses via the use of inclined magnetic springs. Quasi-static and dynamic system models which informed the design process are presented, as well as a finite-element model aimed at validating the assumptions of the quasi-static system model for a select set of system states. Challenges related to the conflicting design requirements of stability, low transmissibility and load-independent resonance frequency are addressed, and an experimental framework for testing the real prototype is outlined.

## INTRODUCTION

The main purpose of a vibration isolation table is to limit the transmission of vibration from the environment through the base to the isolated platform. While this is often accomplished with mechanical springs, these exhibit a natural trade-off between low stiffness (good isolation) and high load bearing capacity (requiring higher stiffness). Also, the linear force-displacement relationship of mechanical springs means that resonance frequency (proportional to the square root of the effective mass loading on the isolated platform) varies directly and sometimes dramatically with changing load.

Theoretical modelling at the University of Adelaide has demonstrated that the use of oblique magnet pairs in place of mechanical springs may help to overcome both of these constraints, due to the nonlinear force-displacement relationship between pairs of magnets (Robertson et al., 2011). This modelling is sufficiently complete to enable it to be utilised in the design and build of a prototype aimed at establishing proof-of-concept of load-independent vibration isolation. Successful demonstration of such a prototype would validate the modelling and represent a new type of vibration isolator with improved performance over commercially available systems.

This paper commences by examining existing literature and modelling formalising the forces between permanent cuboid magnets, the specific application of magnetic levitation for vibration isolation, and the appropriateness of inclined permanent magnetic springs for this application. A theoretical design for a magnetic levitation vibration isolator with a load-invariant resonance frequency is detailed through both quasi-static and dynamic modelling, and an experimental framework for testing the real prototype is outlined.

## FORCES BETWEEN MAGNETS

Linear mechanical springs exhibit a linear force-displacement relationship and constant stiffness for a given load. This allows the differential equations which govern the dynamics

of a mechanical spring system to be solved comparatively simply, however it restricts the possible applications of the spring. The force acting between two permanent magnets or electromagnetic coils due to their magnetic fields has a magnitude which is approximately inversely proportional to the square of the displacement. Using this force-displacement relationship in place of that of the linear mechanical spring, we have a magnetic spring which has a varying stiffness with the deflection of the spring.

Through the manipulation of the magnetic field via electromagnetic coils, the magnetic spring stiffness can be controlled and performance can be improved far beyond what is possible with a passive mechanical spring. The calculation of forces between magnets and coils due to magnetic field interaction, however, presents a far more complex problem. In order to design and/or control the spring, it is necessary to first determine the force-displacement relationship between magnets.

Interaction forces between permanent magnets can be computed numerically using finite element analysis, a method particularly suited to solving for forces between magnets of irregular shape where analytical techniques are too difficult (Akoun & Yonnet, 1984). In cases where an analytical solution exists, finite element analysis is a useful way of validating the solution. Cases where an analytical solution exists include the analysis of more regularly shaped magnets such as cuboid (Akoun & Yonnet, 1984) or cylindrical magnets (Ravaud et al. 2010; Vokoun et al. 2009). These problems can vary in complexity depending on shape, orientation and position with respect to other magnets. Forces between cuboid or cylindrical magnets are of particular interest because magnets of these shapes are readily available and (as practical consideration) easily mounted in a prototype configuration. Cuboid magnets present the simplest analysis, while cylindrical magnets require a more complex method. In the case of actively controlled vibration isolators, it is also of interest to model the forces between magnets and coils in order to enable control of the magnetic spring via magnet-coil actuators.

Akoun and Yonnet (1984) provide a method for calculating forces between cuboid magnets with parallel magnetisation vectors. The algorithm presented by Akoun and Yonnet (1984) is shown below in Equation (1). In order to calculate the force in the  $x$ -,  $y$ - or  $z$ -direction the relevant equation for  $\phi$  (Equation 2, 3 or 4) is substituted into (1). These equations were utilised by Robertson et al. (2011) in the theoretical design of a magnetic spring (discussed later):

$$F = \frac{J \cdot J'}{4\pi\mu_0} \sum_{i=0}^1 \sum_{j=0}^1 \sum_{k=0}^1 \sum_{l=0}^1 \sum_{p=0}^1 \sum_{q=0}^1 (-1)^{i+j+k+l+p+q} \phi(u_{ij}, v_{kl}, w_{pq}, r) \quad (1)$$

(1)

$$\phi_z = \frac{1}{2}(v^2 - w^2) \ln r - u + uv \ln r - v + vwtg^{-1} \frac{uw}{rw} + \frac{1}{2}ru \quad (2)$$

$$\phi_y = \frac{1}{2}(u^2 - w^2) \ln r - v + uv \ln r - v + uwtg^{-1} \frac{uw}{rw} + \frac{1}{2}rv \quad (3)$$

$$\phi_x = -uw \ln r - u + uv \ln r - v + uwtg^{-1} \frac{uw}{rw} + rw \quad (4)$$

where the parameters  $u_{ij}$ ,  $v_{kl}$ ,  $w_{pq}$  and  $r$  are defined by:

$$u_{ij} = \alpha + (-1)^j A - (-1)^i a$$

$$v_{kl} = \beta + (-1)^l B - (-1)^k b$$

$$w_{pq} = \gamma + (-1)^q C - (-1)^p c$$

$$r = (u_{ij}^2 + v_{kl}^2 + w_{pq}^2)^{\frac{1}{2}}$$

Dimensions  $A$ ,  $B$ ,  $C$ ,  $a$ ,  $b$ ,  $c$  and offsets  $\alpha$ ,  $\beta$ ,  $\gamma$  are defined in Figure 1.

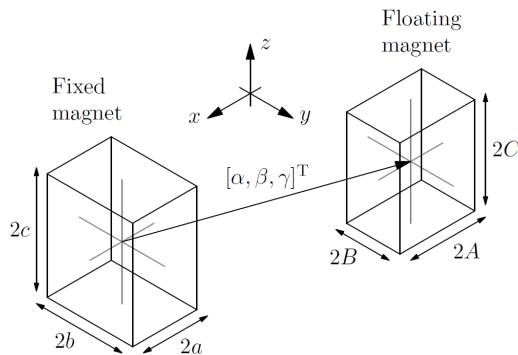


**Figure 1** Dimensions and offsets of cuboid magnets used in equations (1) to (4)

## MAGNETIC LEVITATION FOR VIBRATION ISOLATION

The use of repulsive magnetic springs allows the design of a vibration isolator with a load-independent resonance frequency. Certain arrangements of magnetic springs also allow low stiffness to be achieved without sacrificing load-carrying capacity of the isolator (Zhou & Liu, 2009). This is a direct result of the nonlinear force-displacement relationship between permanent magnets, and has been previously explored for various system configurations including quasi-zero stiffness designs (Mizuno et al., 2006; Carella et al., 2008; Zhou & Liu, 2009; Robertson et al., 2009) and designs incorporating inclined permanent magnet pairs (Robertson, Cazzolato & Zander, 2011). Of these works, it is the latter which is of the most interest to this project, as it has not been demonstrated in a working prototype to date.

Motivation for achieving effective vibration isolation in the low frequency range (<40 Hz) is drawn from the application of laser interferometry, in which multistage vibration isolation systems have previously been used to attenuate problematic low-frequency seismic noise. Design of such multiple-degree-of-freedom vibration isolation systems represents a significant challenge (Richman et al., 1998). A multiple-degree-of-freedom vibration isolation system using magnetic springs may allow for simpler realisation of a load-independent isolation system which is effective in the low-frequency range.

## Inclined Permanent Magnet Pairs

Theoretical models developed by Robertson, Cazzolato & Zander (2011), which built upon and were validated using the results of Akoun and Yonnet (1984), show that a load-independent resonance frequency may be achieved (in the vertical direction only) for relatively simple arrangements of inclined cuboid permanent magnets in repulsion (see Figure 2).

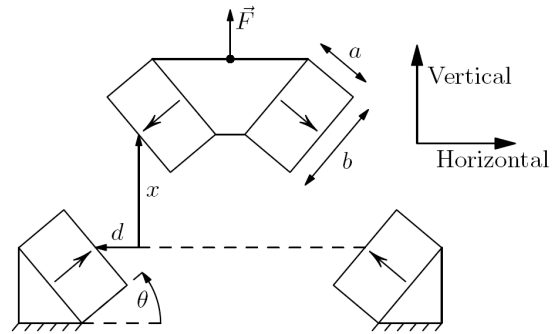


**Figure 2** Theoretical arrangement for a magnetic spring using inclined permanent magnet pairs. “Horizontal” refers to the local  $x$ -axis and “Vertical” to the local  $y$ -axis (Robertson, Cazzolato & Zander, 2011)

In order to define the configuration of the system and subsequently assess performance, several parameters are required including the magnet angle,  $\theta$  and the vertically applied force,  $\vec{F}$ . In addition, three non-dimensional parameters related to the magnet volume,  $V$ , face length,  $b$ , magnet thickness,  $a$  and magnet vertical separation,  $d$  are used to describe the system and are defined as follows:

Unit length,  $u = \sqrt[3]{V}$ , magnet size ratio,  $\gamma = \frac{a}{b}$  and gap ratio,  $g = \frac{d}{u}$ .

The MATLAB-based models developed by Robertson, Cazzolato & Zander (2011) allow evaluation of performance across a wide range of values for each of the design parameters listed above, and are freely available on the internet for academic use.

## STABILITY

While it has been conclusively proven that no configuration of fixed permanent magnets can result in levitation which is fully stable in all rotational and translational degrees of freedom, various methods of stabilisation are feasible. These include forms of stability which require one or more elements of the system to be in motion; a subset of this type of

stabilisation is spin-stabilisation in which one magnetic ring levitates stably above another as long as the floating ring is rotating with a sufficient angular velocity about its axis relative to the fixed ring (Bassani, 2006).

The methods of stabilisation most appropriate to the design of a levitating magnet vibration isolator are mechanical stabilisation and electro-magnetic active control methods. Mechanical stabilisation consists of fixing one or more degrees of freedom of a levitating system, usually those which are the least stable. In this way, only inherently stable translations or rotations of the levitating object are allowed, eliminating the danger of instability. For vibration isolation applications, however, mechanical stabilisation may be undesirable as mechanical coupling may occur between the platform to be isolated and the base or environment via the mechanical constraints, causing unwanted transmission of vibration and reducing the effectiveness of the isolation.

If completely non-contact stable magnetic levitation is desired, active control methods which utilise relative displacement feedback, electromagnetic actuators and a suitable control algorithm must be employed.

### MAGLEV PROTOTYPE

In order to demonstrate the advantages of using inclined permanent magnetic springs for vibration isolation, a prototype magnetic levitation vibration isolator (or “MagLev” device) was developed. The primary goal was the achievement of a load-independent resonance frequency across a specified load range in a passively stabilised (mechanically constrained) configuration, with a view to later incorporating active control methods for fully non-contact levitation.

The prototype configuration consisted of a fixed base frame and a “levitating” platform, coupled through three sets of four inclined permanent magnets (such as the set of four shown in Figure 1). The orientation and position of the magnet pairs is depicted in Figure 3. This configuration was selected through early experimental prototyping to be a stable, easily realisable arrangement which would perform effectively and safely across specified load range of approximately 5 – 20 kg (this range was chosen to be within the safe range of lifting for a single person for reasons of practicality). The mechanical constraints include a self-centring rotational bearing and a low-friction linear recirculating ball bearing, allowing the platform to translate in the  $z$ -direction and rotate about the  $x$ -axis with respect to the base. This two-degree-of-freedom system is stable without requiring any active control methods or actuators.

Safety limits in the form of stoppers are implemented to restrict the movement of the platform in case of sudden or unexpected instability. These limits are adjustable, but are nominally set at  $\pm 5$  mm for translation and  $\pm 5^\circ$  for rotation in each direction.

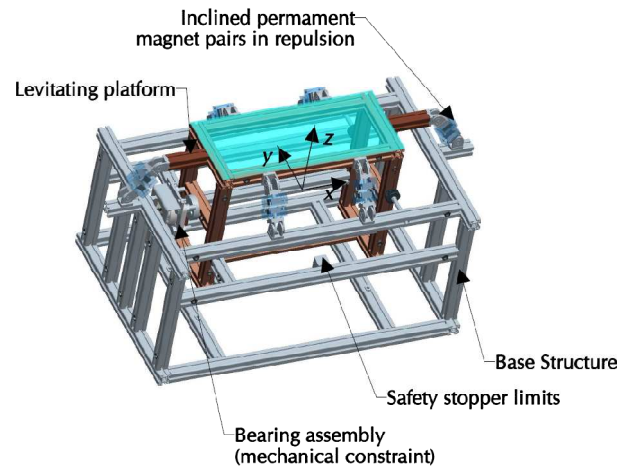


**Figure 3** MagLev device

System operating parameters such as magnet angle and gap ratio are adjustable through the device’s modular design. This is intended to allow rapid prototype modification and optimisation of performance in response to testing and modelling results.

All structural members are constructed out of aluminium, and all components and fasteners in the immediate vicinity of the magnets are either aluminium or marine-grade 316 stainless steel. This is to ensure minimal interference between the supporting structure and the magnetic fields necessary for the prototype’s operation.

### Early design modelling

Initially, a modified version of the static model developed by Robertson, Cazzolato & Zander (2011) was used to calculate the vertical stiffness at equilibrium for the chosen prototype configuration. This enabled selection of the critical design parameters including magnet size, magnet angle and gap ratio via an iterative design approach.

For a specified range of total platform mass (or total design load—equivalent to the force  $\vec{F}$  in Figure 2, but applied in the negative or downward direction), the design process depicted in Figure 4 was carried out until an acceptably load-independent vertical resonance frequency had been achieved.

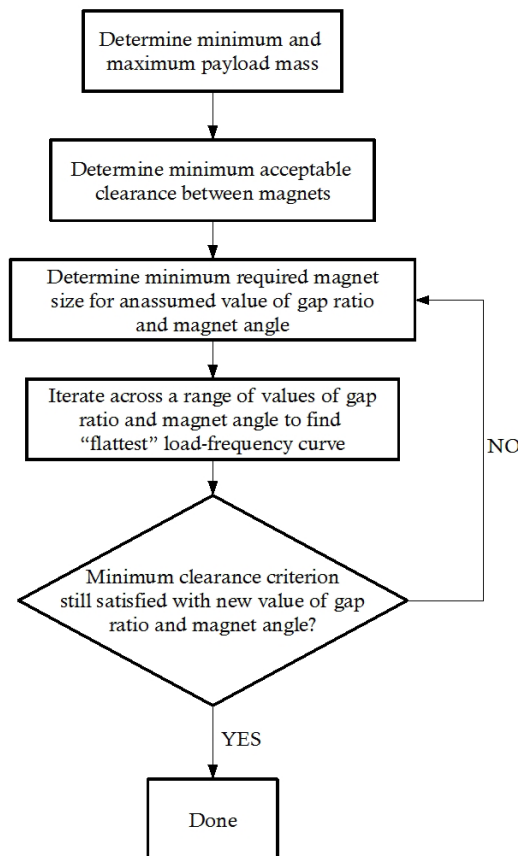


**Figure 4** Magnetic levitation system parameter selection flowchart

The theoretically ideal design parameters determined using the selection process outlined above are detailed in Table 1, and the relationship between vertical resonance frequency and load force  $\vec{F}$  is shown in Figure 5.

**Table 1** Design parameters and performance characteristics of iteratively designed system

Design Parameters	
Magnet length, $a$	25 mm
Magnet width, $a$	25 mm
Magnet thickness, $b$	12.5 mm
Gap ratio, $g$	0
Magnet angle, $\theta$	35°
Expected Performance	
Maximum platform mass, $m_1$	~ 10 kg
Minimum platform mass, $m_2$	~ 5 kg
Nominal vertical resonance frequency, $f_r$	5 Hz
Variation in resonance frequency across mass range ( $z$ -direction), $\Delta f$	~ 0.5%

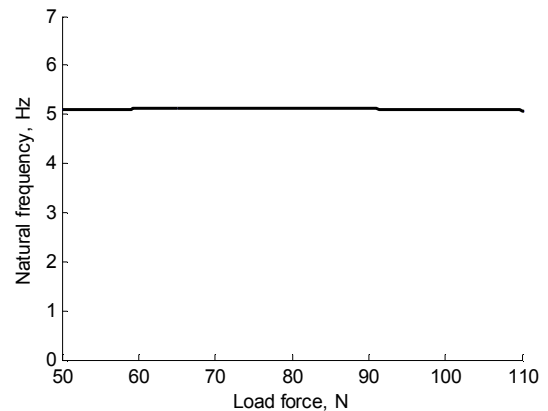


**Figure 5** Vertical natural frequency  $f_n$  versus total load force (platform and payload weight) for ideal system parameters

While a resonance frequency of 5 Hz would seem unacceptably high for an application where extremely low-frequency vibration isolation is desired, Robertson et al. (2011) showed that for such a system, the nominal resonance frequency decreases with increasing magnet volume. This means that scaling the MagLev prototype up (which would be necessary in order to carry heavier loads) would have the added advantage of significantly reducing the system’s natural frequency. For the small-scale MagLev prototype, the primary design goal was the achievement of a load-independent resonance frequency, with the understanding that the low-frequency isolation performance may be improved through active control techniques (which will be attempted at a later stage of development) and scaling up of the prototype (which is beyond the current scope and budget of the project).

**Quasi-static modelling**

In order to understand the force-displacement (stiffness) relationships in each degree of freedom of the MagLev device in more detail, a quasi-static system model was developed using MATLAB. This model leverages some of the “oblique\_forces” code developed by Robertson, Cazzolato & Zander (2011) to calculate the forces and moments between pairs of cuboid magnets, modified to suit the prototype configuration. A given platform position and orientation is passed to the “oblique\_forces” code via appropriate coordinate transformations, where the resultant forces and moments developed between each pair of magnets are calculated. These forces and moments are then returned to the quasi-static model after being transformed to the global coordinate system. The quasi-static model then returns the total force and moment applied to the platform via summation of forces and moments developed between each of the opposing magnet pairs.

**Finite element modelling**

A significant assumption implicit in the use of Robertson’s “oblique\_forces” model was that the moments caused by relative rotation of the magnets are negligible (Robertson’s “oblique\_forces” code cannot calculate the forces or moments between magnets with non-parallel faces due to its use of Akoun & Yonnet’s method of analysis which is restricted to magnets with parallel magnetisation vectors). That is, for each floating magnet, the moment exerted on the platform about its centre of rotation due to the misalignment of that magnet’s face with the face of the corresponding fixed

magnet is insignificant in magnitude when compared to the lever arm moment resulting from the translation of that magnet about the platform's centre of rotation. This is more formally represented in the following assumption and applied to the quasi-static model: for small rotations of the floating platform, the face of each floating magnet can be assumed to remain parallel to the face of the corresponding fixed magnet.

This small-angle assumption was implemented in the quasi-static model in that rotations of the platform result in translations of the rotating magnets about the centre of rotation, but not rotations of the magnets themselves. This assumption is depicted in Figure 6. This assumption significantly eased the development of the quasi-static model (and, later, the dynamic model) in that it allows direct utilisation of Robertson's code as a nested function call and reduces the required computational effort.

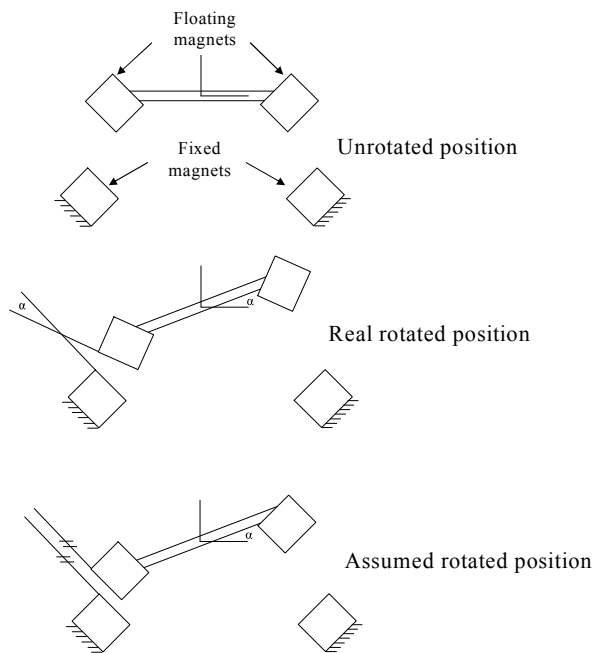


**Figure 6** Small angle assumption used in quasi-static model

Finite element modelling investigated the small angle assumption by comparing a simplified set of four cuboid magnets with and without the small angle assumption applied. The simplified model consisted of two fixed and two floating magnets and specifically compared global moments for changes in angle rotation of the platform.

The validity of the small-angle assumption was found to be largely dependent on the vertical separation between the fixed and floating magnets (and therefore the total platform loading) and the location of the axis of rotation of the platform. Locating the platform's axis of rotation in the same plane as the centres of the floating magnet faces (as in Figure 6) resulted in an error in moment estimation via the small angle assumption of less than 3% compared to real rotation (across a range of total platform rotation of 0°-5°). Moving the axis of rotation of the platform downward by 150 mm increased this error up to 40% at 5 degrees of rotation. However, the error in moment estimation via the small-angle assumption was always less than 2% for very small angles of rotation (less than 1°).

All of the above suggests that use of the developed quasi-static model in an actively stabilised configuration may

represent a significant challenge due to the inherent error in the assumptions utilised to simplify the modelling. However, for very small rotations the model has been found to be valid, and for larger rotations, it may be possible to utilise adaptive control techniques to overcome the poor estimates of total moment by the model.

Finite element modelling also revealed that platform configurations with a gap ratio of zero presented a stability issue. A gap ratio of zero means that the two pairs of magnets depicted in Figure 2 are positioned such that each floating magnet is located directly above the corresponding fixed magnet at the equilibrium position ( $d=0$  in Figure 2). In this configuration, the eccentricity of the centre of rotation of the platform with respect to the plane in which the floating magnets are mounted results in a negative stiffness in this rotational degree of freedom, and therefore instability. However, this effect is masked by the small-angle assumption, and therefore does not appear in the quasi-static modelling even for a gap ratio of zero.

As was seen in Table 1, the configuration resulting in the best achievable performance (i.e. load-independent resonance frequency) included a gap ratio of zero. As discussed above, however, this gap ratio was shown to be an unstable configuration when modelled using finite element analysis. In order to rectify the above stability issue, it was required to select a value of gap ratio greater than zero or mechanically constrain the rotational degree of freedom. A high degree of stability is desirable in this degree of freedom because it reduces the number of constraints (and therefore the potential for mechanical coupling) which must be applied to the platform, and will also reduce the required control effort when active stabilisation is applied.

In light of this, a new gap ratio of 0.5 was chosen to improve the system's stability in rotation about the  $x$ -axis. The relationship between total platform loading and vertical resonance frequency with the new value of gap ratio is shown for several values of magnet angle in Figure 7, below.

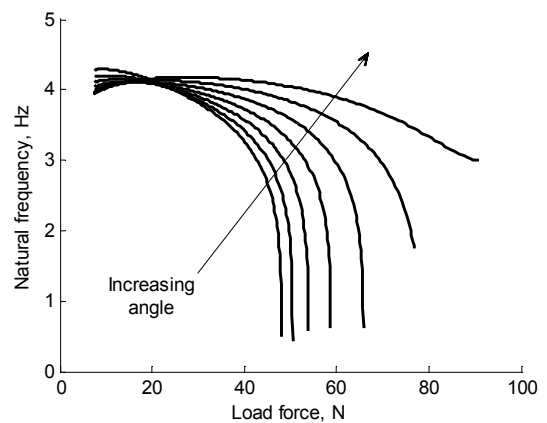


**Figure 7** Natural frequency versus load force for gap ratio of 0.5 and magnet angles from 35° to 65° in increments of 5°

As can be in Figure 8, selection of an appropriate magnet angle (in this case 60°) allowed an acceptably load-independent resonance frequency to be achieved, even with a nonzero gap ratio. The total variation in resonance frequency across the load range was approximately 1.2% for the new gap ratio, but this increase was considered an acceptable tradeoff in order to ensure stability in rotation about the  $x$ -axis.

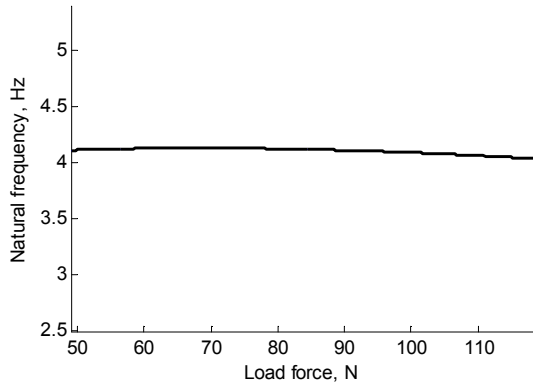


**Figure 8** Natural frequency versus load force for gap ratio of 0.5 and magnet angle of 60°.

**Dynamic modelling**

Once the quasi-static model had been developed, it could be used as a MATLAB function block in a dynamic SIMULINK model, shown in Figure 9. This model reads in the platform position at the current timestep and generates a resultant force and moment in each degree of freedom via the quasi-static model function block. These forces and moments are used to generate linear and angular accelerations of the platform relative to the base, which are then integrated twice to obtain the new platform position. This new platform position is fed back into the quasi-static model at the next timestep, and used to generate new forces and moments.

A particular limitation of the quasi-static model is that the isolator’s base is assumed to remain fixed; the only relative motion between the base and platform is assumed to occur at the platform. This is obviously a drawback when attempting to calculate displacement transmissibility between the base and platform. In order to overcome this limitation, the platform position was simply biased by a time-variant signal equal to the base excitation, and the resultant forces on the platform were calculated based on its relative position with respect to the base.

The technique described above allows displacement transmissibility between the base and platform to be satisfactorily calculated, but neglects the additional damping caused by the relative movement of the base (damping is applied proportionally to the absolute platform position). Modification of the dynamic model to include the real effect of the moving base is planned if this inaccuracy in the damping term proves problematic. As will be discussed later, however, the values of damping used in the dynamic modelling were only rough approximations due to the complex nature of modelling eddy current damping in moving magnetic fields.

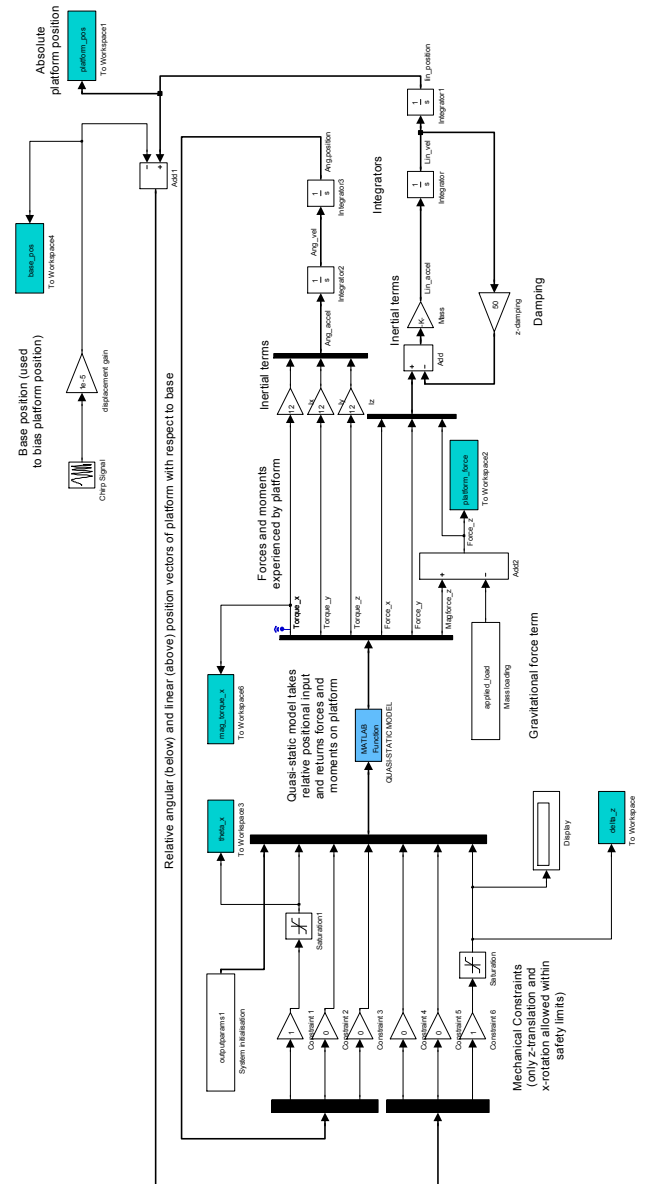


**Figure 9** MagLev system dynamic SIMULINK model

**Damping**

Due to the non-contact nature of a levitating magnet vibration isolator, mechanical damping is usually not present. However, as discussed by Sodano et al. (2006), a form of electromagnetic damping does exist called eddy-current damping. Eddy currents occur when a magnetic field is in motion relative to a nonmagnetic conductive structure (such as aluminium). The moving magnetic field induces current to flow in the conductor with an opposite polarity to the inductive field. This results in a magnetic force which opposes the motion of the moving field and has a magnitude proportional to the relative velocity between the field and conductor. This energy is eventually dissipated as heat in the structure. Such damping is roughly analogous to the viscous mechanical dampers found in traditional vibration isolators, and is likely to have a similar effect on the vibration isolation performance of the MagLev device. While eddy current damping was not a design aim in the development of the MagLev device and the levels of damping observed in the device are therefore unlikely to be as high as those achieved by Kienholtz et al. (1994), some damping can be assumed to be present. Extensive modelling of these effects was deemed

unnecessary and time-consuming due to the complex geometrical configuration of the structure, and as an assumed damping ratio of 0.025 in the vertical direction was utilised in the preliminary dynamic modelling, with this value to be updated once early test results are obtained. Damping was assumed to be negligible in the rotational degree of freedom for purely vertical excitation, and is therefore not currently included in the model.

**THEORETICAL RESULTS**

In order to calculate the displacement transmissibility of the vibration isolator in the z-direction, a 0.1-50 Hz chirp displacement signal of amplitude  $1 \times 10^{-5}$  m was applied to the base. The frequency range of 0.1-50 Hz was selected as this encompasses the entire frequency range identified by Richman et al. (1998) as being of interest for applications of laser interferometry (0.15-40 Hz). The transmissibility between the base displacement (“base\_pos” in Figure 9) and the platform absolute displacement (the z-component of “platform\_pos” in Figure 9) was then determined, along with the coherence. These relationships are shown in Figures 10 and 11, respectively. All of the figures in this section were generated using Welch’s method for FFT estimates via a Hanning window with 4096 samples, 75% overlap and a sampling frequency of 1000 Hz (10 FFT averages).

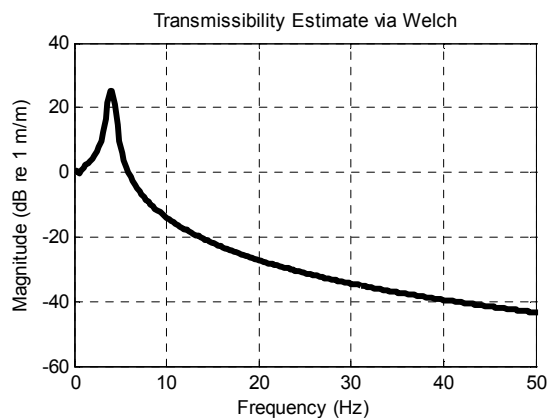


**Figure 10** Simulated vertical transmissibility of isolator

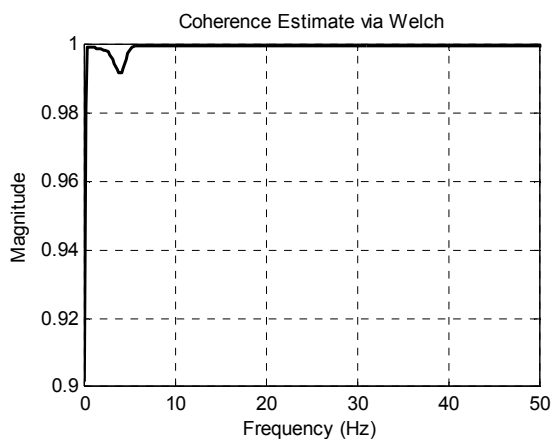


**Figure 11** Simulated vertical coherence of isolator

As can be seen in Figure 10, a resonance peak exists at approximately 4 Hz, as expected. A dip in coherence is observed at resonance, consistent with the theoretical expectations of a nonlinear plant operating in the large-displacement range. This drop in coherence is small enough

to be negligible however, for the displacement ranges of interest. It was attempted to increase the input gain in order to determine whether the coherence would degrade further with greater displacement, but no significant change in coherence was observed for displacements within the allowable range ( $\pm 5$  mm in the z-direction). This indicates that use of a linear controller, configured at the selected platform operating point (for a specified mass loading), should be sufficient for vertical vibration control.

**PROPOSED EXPERIMENTAL METHODOLOGY**

In order to validate the design modelling and evaluate the performance of the MagLev prototype, both quasi-static and dynamic testing is planned. The results of these tests will be used to assess not only the performance of the prototype, and also the operating characteristics which could not be determined through modelling alone (such as the effective magnitude of the eddy current damping in each degree of freedom). The experimental results from the passively stable prototype will inform the design of the control system for the actively stabilised, wholly non-contact prototype configuration.

**Quasi-static testing**

As a validation of the quasi-static modelling, single-axis forces and moments will be applied to the levitating platform via a six-degree-of-freedom load cell. The reaction force or moment due to the interaction of the magnetic springs measured by the load cell will be correlated with six-degree-of-freedom ultrasonic head tracker made by Logitech. The force- and moment-displacement relationships in both of the prototype’s two degrees of freedom will be compared to the expected results from the quasi-static model. Where necessary, the quasi-static model will be corrected to compensate for possible minor differences in modelling constants (such as actual versus expected values of magnetisation strength of the cuboid magnets).

**Dynamic testing**

The base of the MagLev prototype will be subjected to an input force with a random white noise source and/or chirp signal to test for transmissibility, resonance and stability of the base-platform system over varying payload masses. The input force is to be provided by a large electrodynamic shaker, capable of delivering up to 250 N of force across a frequency range of up to 5 kHz and a total stroke length of 38 mm. A custom testing rig has been designed to house the shaker and allow excitation of a range of test specimens including the MagLev prototype (see Figure 12).

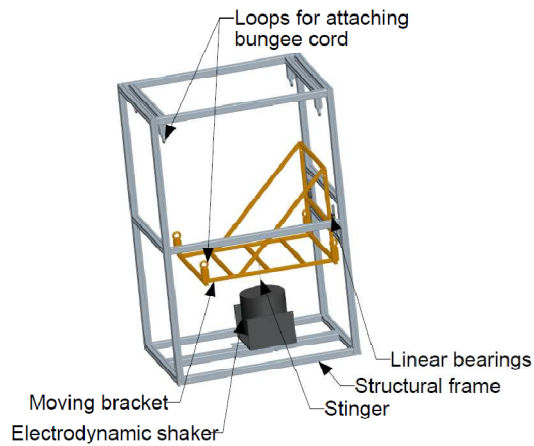


**Figure 12** Testing apparatus incorporating electrodynamic shaker

In the testing rig, an elastic bungee cord supports the weight of the moving bracket which holds the test specimen, such that the shaker must only apply the force necessary to produce the desired acceleration. Linear bearings constrain the moving bracket to a single translational degree of freedom so as to protect the shaker from damaging moments. However, the entire test rig may be turned on its side in order to cause excitation in the horizontal direction.

The position of the shaker underneath the moving bracket is adjustable such that the stinger may be positioned to act directly through the centre of gravity of the device to be tested. This is important for the MagLev prototype to ensure that the purely vertical mode can be excited in testing in order to reproduce the conditions of the modelling as faithfully as possible. In testing of the fully active (non-contact) prototype, it is planned to excite the device in both the vertical and horizontal directions.

In order to measure the system's vertical transfer function across the specified frequency range, two accelerometers will be used. One will be placed on the base structure and one on the platform as close as possible to the axis of rotation to avoid cross-coupling with the rotational degree of freedom (and thereby distortion of the results). The experimental results will be compared with those obtained through the modelling, and system and model parameters corrected accordingly.

Structural resonances from the aluminium framing of both the MagLev prototype and testing rig are expected to be at high enough frequencies so as to couple minimally with the planned low-frequency testing.

## CONCLUSIONS

Theoretical modelling has shown that the realisation of load-independent resonance frequency is feasible for a vibration isolator using inclined cuboid permanent magnet springs. The MagLev prototype is under construction, with the passively stable configuration to be tested shortly. While the resonance frequency of the prototype is too high to be used effectively for low frequency applications such as laser interferometry, it is expected that active vibration control in the vertical direction will allow the resonance frequency in this direction to be driven much lower, and therefore make the system much more appropriate for such an application (as would scaling up the volume of the magnetic springs).

Once the passively stable prototype has been successfully demonstrated and tested to validate the modelling, it is planned to implement active non-contact stabilisation (true levitation) through the use of electromagnetic actuators.

Some nonlinearity exists in the plant due to the inherent nonlinear force-displacement relationship of the magnetic springs, but it is expected that for small displacements the plant can be assumed to behave linearly at frequencies far from resonance, and adaptive control techniques may also be implemented to overcome the nonlinearity issues if operation over larger displacement ranges is required.

## ACKNOWLEDGEMENTS

The authors gratefully acknowledge the Australian Acoustical Society, Dr. Carl Howard (AAS), the University of Adelaide School of Mechanical Engineering and Open Day Innovation Fund for their funding and in-kind support of this project.

## REFERENCES

- Akoun, G and Yonnet, J 1984, "3d analytical calculation of the forces exerted between two cuboidal magnets," *IEEE Transactions on Magnetics*, vol. 20 no. 5, pp. 1962-1964.
- Bassani, R 2006, "Earnshaw (1805-1888) and passive magnetic levitation," *Meccanica*, vol. 41 no. 4, pp. 375-389.
- Carella A, Brennan, MJ, Waters, TP and Shin, K 2008. "On the design of a high-static-low-dynamic stiffness isolator using linear mechanical springs and magnets," *Journal of Sound and Vibration*, vol. 315 no. 3, 712-720.
- Kienholtz, DA, Pendleton, SC, Richards, KE and Morgenthaler, DR 1994, "Demonstration of solar array vibration suppression," In *Proceedings of SPIEs Conference on Smart Structures and Materials*, pp. 59-72, Orlando, Florida, February 14-16.
- Mizuno, T Takasaki, M, Kishita, D and Hirakawa, K 2006. "Vibration isolation system combining zero-power magnetic suspension with springs," *Control Engineering Practice*, vol. 15 no. 2, pp. 187-196.
- Ravaud, R, Lemarquand, G, Babic, S, Lemarquand, V, and Akyel, C 2010, "Cylindrical magnets and coils: Fields, forces, and inductances," *IEEE Transactions on Magnetics*, vol. 46 no. 9, pp. 3585-3590.
- Richman, SJ, Giaime, JA, Newell, DB, Stebbins, RT, Bender, PL and Faller, JE 1998, "Multistage active vibration isolation system," *Review of Scientific Instruments*, vol. 69 no. 6, pp. 2531-2538.
- Robertson, W, Kidner, M, Cazzolato, B and Zander, A 2009, "Theoretical design parameters for a quasi-zero stiffness magnetic spring for vibration isolation," *Journal of Sound and Vibration*, vol. 326 no. 1-2, pp. 88-103.
- Robertson, W Cazzolato, B and Zander, A 2011, "Inclined permanent magnets for a translational spring with load independent resonance frequency and low stiffness", *Journal of Sound and Vibration*, under review.
- Sodano, HA, Bae, JS, Inman, DJ and Belvin, WK 2006, "Improved concept and model of eddy current damper," *Journal of Vibration and Acoustics*, vol. 129 no. 3, pp. 295-302.
- Zhou, N and Liu, K 2009, "A tunable high-static-low-dynamic stiffness vibration isolator," *Journal of Sound and Vibration*, vol. 329 no. 9, pp. 1254-1273.
- Vokoun, D, Beleggia, M, Heller, L and Sittner, P 2009, "Magnetostatic interactions and forces between cylindrical permanent magnets", *Journal of Magnetism and Magnetic Materials*, vol. 321 no. 22, pp. 3758-3763.